ACS OMEGA

http://pubs.acs.org/journal/acsodf

Article

Protective Action of *Jania rubens* Nanoencapsulated Algal Extract in Controlling Vegetable Oils' Rancidity

Yasmin R. Maghraby,* Mohamed A. Farag, and Adham R. Ramadan

Cite This: *ACS Omega* 2021, 6, 5642−5652

Read Online

ACCESS | Metrics & More | Article Recommendations | Supporting Information

ABSTRACT: The development of natural antioxidants that can mitigate oil oxidation is on the rise. Several antioxidants have been developed from natural terrestrial plants, with less emphasis on marine algae. Rancidity is a major degradative reaction limiting the shelf-life and deteriorating the quality of vegetable oils. The goal of this study was to evaluate the ability of the *Jania rubens*' (*J. rubens*) seaweed extract encapsulated by chitosan/tripolyphosphate in retarding lipids' oxidation in vegetable oils. To improve the *J. rubens* efficacy, the extract was nanoencapsulated using the ionic gelation method. A Box−Behnken design was applied for the optimization of the formulation variables (chitosan/tripolyphosphate amounts, homogenization time, and homogenization speed). The optimum nanoformulation was characterized by transmission electron microscopy. It had a particle size of 161 nm, zeta potential of 31.2 mV, polydispersity index of 0.211, and entrapment efficiency of 99.7%. The ability of the optimum formula to extend the shelf-life of vegetable oils was based on peroxide value and thiobarbituric acid assays. In addition, headspace solid-phase microextraction was applied to detect the oils' volatiles as secondary markers of rancidity. The results revealed that the nanoencapsulated algal extract considerably reduced the rate of oils' oxidation and that its activity was comparable to that of a widely used synthetic antioxidant.

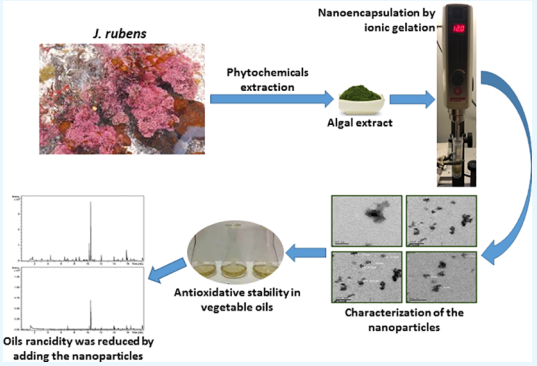

INTRODUCTION

Lipid oxidation is a major degradative reaction limiting the shelf-life and deteriorating the quality of lipid-containing food products.[1] The oxidative deterioration of food products has a negative impact in the food industry in addition to the generation of potentially toxic products.[2] Consequently, the inclusion of additives to slow down or stop the propagation of oxidation reactions is warranted, especially for prolonged storage durations.[3] Currently, there is increasing interest in using natural phytochemicals with potential antioxidant activity due to their ability to retard oxidation reactions and to extend food's shelf-life.[4]

Seaweeds are an important source of bioactive compounds that could potentially be exploited as functional ingredients in food.[5] Seaweeds represent an excellent source of vitamins (A, D, and E),[6] antioxidants (polyphenols and fatty acids),[7] and minerals (Ca, P, and Na).[8] Among the various common seaweed species found along the Mediterranean coast, the red algae *Jania rubens* (*J. rubens*) is rich in several bioactive compounds including flavonoids, vitamins, and fatty acids.[9,10] These chemicals can be used as additives in food products, supplements, cosmetics, etc.[11]

Nevertheless, the incorporation of crude algal extracts into food products can be limited due to their astringent taste, high reactivity with other food components, poor solubility, long-term instability, and fast sedimentation.[12] Consequently, nanoencapsulation presents a potential solution to mask the phytochemicals' astringent taste typical in tannins, preserving the food's sensory properties concurrent with improved stability and activity of the entrapped phytochemicals.[13] Nanoencapsulation could also protect the bioactive compounds from light/oxygen and improve their dispersibility in food systems.[4] The bioactive compounds' carrier material must be of a food-grade type and should also be stable in food systems, i.e., during processing, packaging, and storage.[14] Accordingly, the most suitable nanocarrier materials for food applications are carbohydrate-based carrier materials.[15] These are biocompatible/biodegradable and can interact with a wide range of bioactive compounds via their functional groups.[16] Additionally, carbohydrate-based delivery systems are considered a suitable shell under elevated temperature processes due to their thermal stability.[17] Chitosan (CS) is a natural polysaccharide and is of common use due to its recognition as generally recognized as safe (GRAS) by the United States Food and Drug Administration.[18] Properties such as *in situ* gelation, biodegradability, biocompatibility, and nontoxicity

Received: December 15, 2020
Accepted: January 19, 2021
Published: February 15, 2021

https://dx.doi.org/10.1021/acsomega.0c06069
ACS Omega 2021, 6, 5642−5652

make CS suitable for usage in food application.[19] Latest reports indicate that an entire CS nanoparticle (NP) can be taken up by human cells, significantly enhancing the bioavailability of the entrapped phytochemicals.[20]

In the present study, *J. rubens* chitosan nanoparticles (JCNP) were prepared by an ionic gelation technique using sodium tripolyphosphate (TPP) as the cross-linking agent with the aim of increasing the stability and activity of the entrapped phytochemicals in food products. A three-factor three-level Box−Behnken design (BBD) was applied to study the effects of the different variables on the studied responses with the target of producing an optimized formula entrapping the *J. rubens*' extract. The optimum formula was characterized by transmission electron microscopy (TEM). Corn, sunflower, soybean, and palm oils were used as oil model systems monitored by determining primary and secondary oxidation products. In addition, to confirm the antioxidative action, the volatiles of the oxidized oils were monitored as markers of rancidity.

RESULTS AND DISCUSSION

Formulation Optimization by 3^3 BBD. The responses of PS (Y1), ZP (Y2), PDI (Y3), and EE % (Y4) were fitted individually to linear, two-factor interaction, and quadratic models using linear regression to obtain the model of choice with the highest adjusted and prediction r^2. ANOVA testing was performed to identify the significant terms of the chosen model on the responses. The model terms with a p value < 0.05 were considered statistically significant. Model reduction was performed by removing the nonsignificant model terms to improve the chosen model and achieve a higher prediction r^2.

The quadratic model was the model of choice for all the four responses since it had the highest adjusted and prediction r^2. After model reduction, the final equations for the responses related to different factors and interactions in terms of coded variables were obtained using the Design Expert software and are as follows:

$$\begin{aligned}\mathrm{PS} = {} & 232.5 - 889.79A + 508.54B - 48.29C \\ & + 1.37D490.75AB + 758.90A^2 + 147.90B^2 \\ & + 39.77C^2 + 227.27D^2\end{aligned}$$

$$\begin{aligned}\mathrm{ZP} = {} & 28.82 + 10A - 9.51B - 0.22C + 0.18D - 0.95AC \\ & - 4.4A^2 + 1.82B^2 + 0.3C^2 - 1.03D^2\end{aligned}$$

$$\begin{aligned}\mathrm{PDI} = {} & 0.21 - 0.17A - 0.13B - 0.022C - 0.018D \\ & - 0.087AB - 0.072AD + 0.2A^2 + 0.026B^2 \\ & + 0.017C^2 + 0.022D^2\end{aligned}$$

$$\begin{aligned}\mathrm{EE\%} = {} & 98.48 - 7.88A + 5.63B - 2.23C + 0.65D \\ & + 2.6AB - 2.33AC + 1.38AD - 1.03BC \\ & + 1.86BD + 3.313CD - 3.79A^2 - 3.17B^2 \\ & - 3.85C^2 - 4.08D\end{aligned}$$

Influence of the Investigated Factors on PS. JCNP must be small enough to control the release of the extract from the NPs in food systems and further inside the human body upon ingestion.[28] The PS of JCNP ranged from 168 nm up to about 2587 nm, suggesting the capacity to produce small NPs (Table S1). ANOVA revealed that the most significant factors affecting PS were the CS percentage (A) and TPP percentage (B), both having a $p < 0.0001$. However, the HT (C) and HS (D) did not have any significant effect on the JCNP PS, having p values of 0.4610 and 0.9832, respectively. Other investigations also showed that the HT and HS had no significant effect on the PS of CS NPs.[29] The 3D surface plot obtained from ANOVA (Figure 1A) showed that increasing both CS (A) and TPP (B) levels was associated with a significant decrease in the PS. However, a further increase in the CS and TPP levels led to an increase in PS. Statistical analysis showed that the optimum JCNP with the smallest PS was obtained at a chitosan/TPP ratio of 2.7:1. Below this ratio, the concentration of CS was not enough to form cross-linked matrices with TPP. With a CS/TPP ratio of 2.7:1, the PS decreased due to an increased density of cross-linking between the CS and TPP.[30] Higher CS/TPP ratios led to larger PS due to accumulations of excess CS molecules on the surfaces of JCNP.[31] In addition, the high availability of TPP could have caused the dominant inter- and intramolecular cross-linkages to be associated with TPP, enabling the NPs to form large flocculating aggregates.[28] In addition, when the CS concentration is high, it approaches the limit of critical concentration of coil overlap where the chains are close to one another, forming connected coils, and then the anionic TPP starts interacting with few cationic groups on the CS chains folding over themselves (mainly through intramolecular links). Moreover, elevating the CS concentration increased the viscosity of the solution, which decreased the diffusion of TPP, forming NPs with big PS.[22]

Influence of the Investigated Factors on ZP. The potential physical stability of any NPs' dispersions is strongly related to their ZP value. The higher the ZP value, the more stable the system becomes.[32] As presented in Table S1, the ZP of the JCNP ranged from 11.3 to 44.0 mV, suggesting the production of NPs with a good physical stability. The positive ZP was due to the presence of CS $-NH^{3+}$ groups. ANOVA showed that the ZP was significantly affected by the CS (A) and TPP (B) percentile levels, as both exhibited very low p values (i.e., $p < 0.0001$). However, the HT (C) and HS (D) had a nonsignificant effect on the ZP, having p values of 0.73 and 0.78, respectively. As shown in Figure 1B, ZP significantly increased by increasing the CS levels due to an increased formation of protonated $-NH^{3+}$ groups on the surfaces of JCNP, which occurred as a result of the acidic pH of the NPs' production steps. In other words, increasing the CS level augmented the overall positive charge of the solution, which consequently increased the ZP value, improving the physical stability of the overall system.[33] Conversely, increasing the TPP concentration led to a decrease in the ZP due to the neutralization of the positively charged $-NH^{3+}$ groups by the TPP negative ions.[34] Last, with an increase in TPP above the critical concentration, the cross-linking salt started occupying most of the positively charged $-NH^{3+}$ groups of CS. Thus, the electrostatic repulsion between the NPs is reduced, and the ZP of JCNP decreased, reducing the physical stability of the colloidal system.[29]

Influence of the Investigated Factors on PDI. The PDI value determines the heterogeneity/size distribution of the prepared NPs, with a PDI < 0.4 being an acceptable value.[21] The PDI of JCNP varied from 0.112 to 0.477, suggesting an acceptable PS distribution and a reproducible

https://dx.doi.org/10.1021/acsomega.0c06069
ACS Omega 2021, 6, 5642−5652

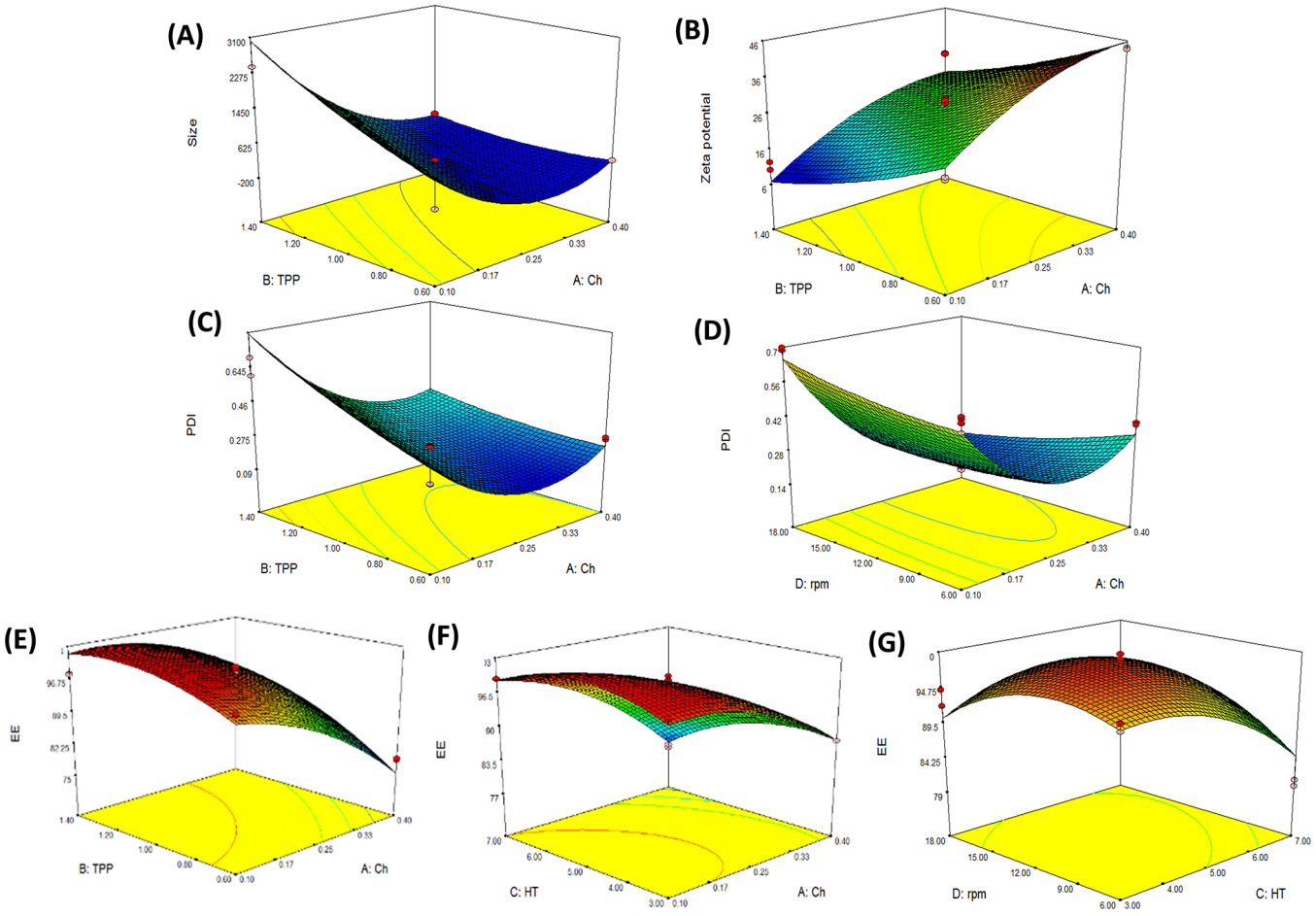

Figure 1. 3D surface plots for the main effects and interactions of CS percentage, TPP percentage, HT, and HS on (A) PS, (B) ZP, (C and D) PDI, and (E–G) EE %.

method of preparation (Table S1). ANOVA revealed that the most significant factors affecting the PDI were the CS (A) and TPP (B) percentile levels, both having a $p < 0.0001$. The HT (C) and the HS (D) did not have a significant effect, with p values of 0.2029 and 0.2969, respectively. The main effects/interactions of the CS and TPP concentrations on the PDI are represented by the 3D surface plot shown in Figure 1C. The PDI decreased by increasing the CS concentration and then it started to increase owing to the electrostatic repulsion taking place between the CS polymer, which could lead to aggregations of some of the CS molecules, thereby forming NPs of different sizes.[35] Nevertheless, increasing the TPP concentration was associated with an increase in the PDI due to the fact that the negatively charged phosphate ions of TPP reacted with the positively charged $-NH^{3+}$ groups of CS and neutralized some of the surface charges, probably leading to the formation of noncompact NPs with a varied size distribution.[34] Although HS independently did not have any significant effect on the PDI, ANOVA showed that HS had an interaction with the CS percentage that affected the PDI significantly. Figure 1D shows the interaction between the CS percentage with the HS and their combined effect on the PDI. The plot shows that by increasing the CS concentration, the PDI decreased and then again started to increase. Meanwhile, increasing HS was associated with an increase in the PDI value due to the cross-linking taking place during the homogenization step.[28]

Influence of the Investigated Factors on EE %. Contrary to PS, PDI, and ZP, ANOVA revealed that three of the studied factors (i.e., CS percentage, TPP percentage, and HT) had a significant effect on the EE %, with $p < 0.0001$. The EE % of JCNP ranged from 77.6% to 99.7%, indicating that the extract was efficiently entrapped into the NPs (Table S1). Primarily, CS carries a positive charge due to the freely available $-NH^{3+}$ groups, and thus electrostatic attraction is created with the negatively charged free algal polyphenolic groups/other anionic phytochemicals, enhancing the EE %.[36,37] CS/TPP interaction significantly affected the EE % of JCNP, having a p value of 0.0142. Increasing the CS percentage led to a decrease in the EE % due to an increased CS viscosity, which might decrease the extract's diffusion inside the NPs' core.[38] Additionally, a high CS concentration might have restricted the phytochemicals' cargo into CS matrices since the possibility of ionic interactions between CS and TPP is decreased.[39] It was also observed from the 3D plot (Figure 1E) that as the TPP levels increased, the EE % subsequently became higher due to the creation of a vast amount of cross-linking TPP networks capable of entrapping diverse bioactive elements.[40]

Figure 1F shows the interaction between the CS levels and the HT to be significant with a p value of 0.0271. As mentioned earlier, increasing the CS levels led to a decrease in the EE % due to an elevated CS viscosity. Moreover, prolonging the HT led to higher EE % values since sufficient

https://dx.doi.org/10.1021/acsomega.0c06069
ACS Omega 2021, 6, 5642–5652

Table 1. Independent Variables and Respective Levels of the 3^3 BBD for JCNP Preparation and Their Levels for the Optimized JCNP Formula

	levels of variables			
factors (independent variables)	low (−1)	medium (0)	high (+1)	optimized level
[A]: CS percentage (w/v)	0.1	0.25	0.4	0.26
[B]: TPP percentage (w/v)	0.6	1.0	1.4	0.96
[C]: HT (min)	3	5	7	4.50
[D]: HS (rpm)	6000	12,000	18,000	1199

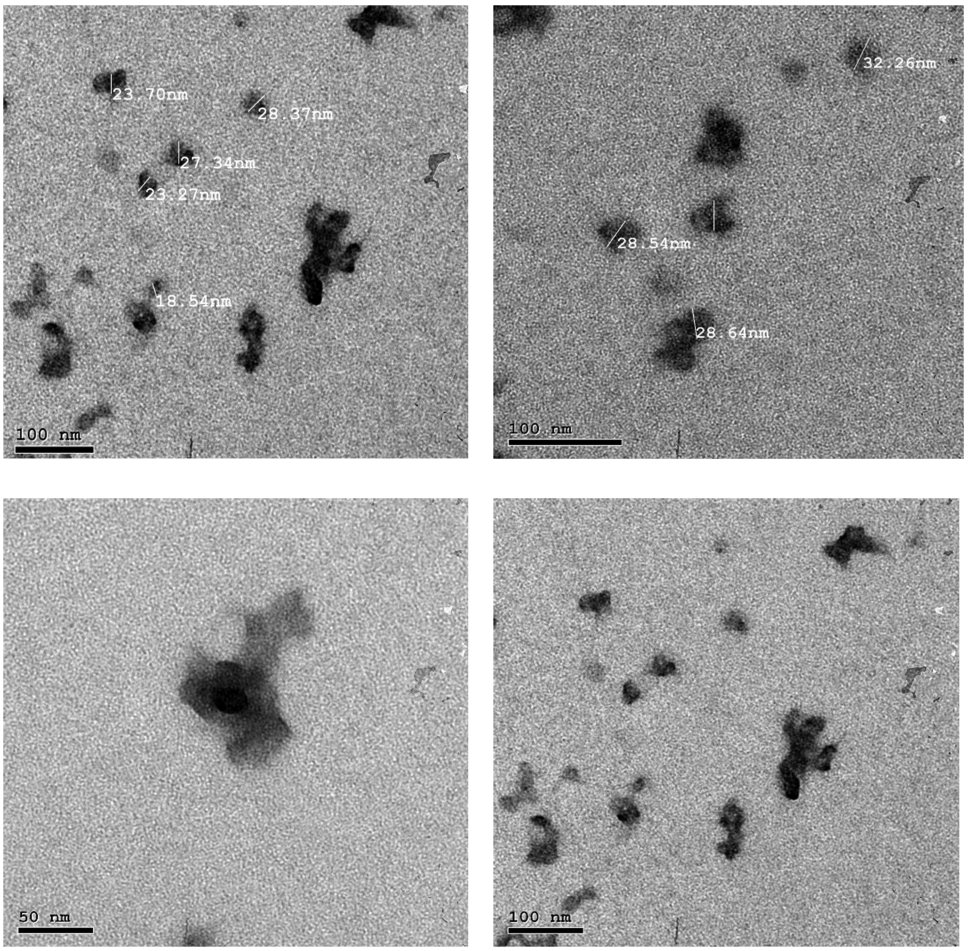

Figure 2. TEM micrographs of the optimized JCNP.

time for the process of entrapment to occur was allowed.[41] However, at higher HT values, the EE % started to decrease, most likely because of the leakage of the phytochemicals from the CS/TPP matrices.[42] Last, ANOVA showed that there is an interaction between both the HT and the HS (having a p value of 0.0037), affecting the EE % (Figure 1G). Prolonging the HT led to an increase in EE %, and then the entrapment efficiency started to decrease due to the reasons explained previously. By increasing the speed, the EE % was initially high due to the enhancement of the cross-linkages between the polymer and the phytochemicals.[41] This could be related to the high potency of CS to form ionic gels at elevated speeds of homogenization, which prevents the leakage of the phytochemicals to the external phase.[41] In other words, an increase in the HS reduced the PS as higher speeds reduce particle aggregations and develop cavitational forces in the homogenization gap, leading to a reduction of the polymers' size with a subsequent drop in the EE %.[43]

Formulation Optimization and Characterization of the Optimized JCNP. After applying constraints on PS, ZP, PDI, and EE %, the optimized formula was identified by the Design Expert software, with an overall desirability of 0.915. The factor levels of the optimized formula are shown in Table 1. The suggested JCNP formula was prepared and evaluated. The validity of the optimization process was confirmed since the observed PS, ZP, PDI, and EE % exist between the low and high confidence intervals of the predicted values, as shown in Table S2.

The PS observed by ultrahigh vacuum TEM was much smaller than that obtained by means of a Zetasizer through a dynamic light scattering technique. TEM images revealed that the PS ranged from 20 to 100 nm. Most of the JCNP were aggregated in the TEM images in accordance to previous studies where CS polymers also tended to form agglomerates (Figure 2).[21,44]

https://dx.doi.org/10.1021/acsomega.0c06069
ACS Omega 2021, 6, 5642−5652

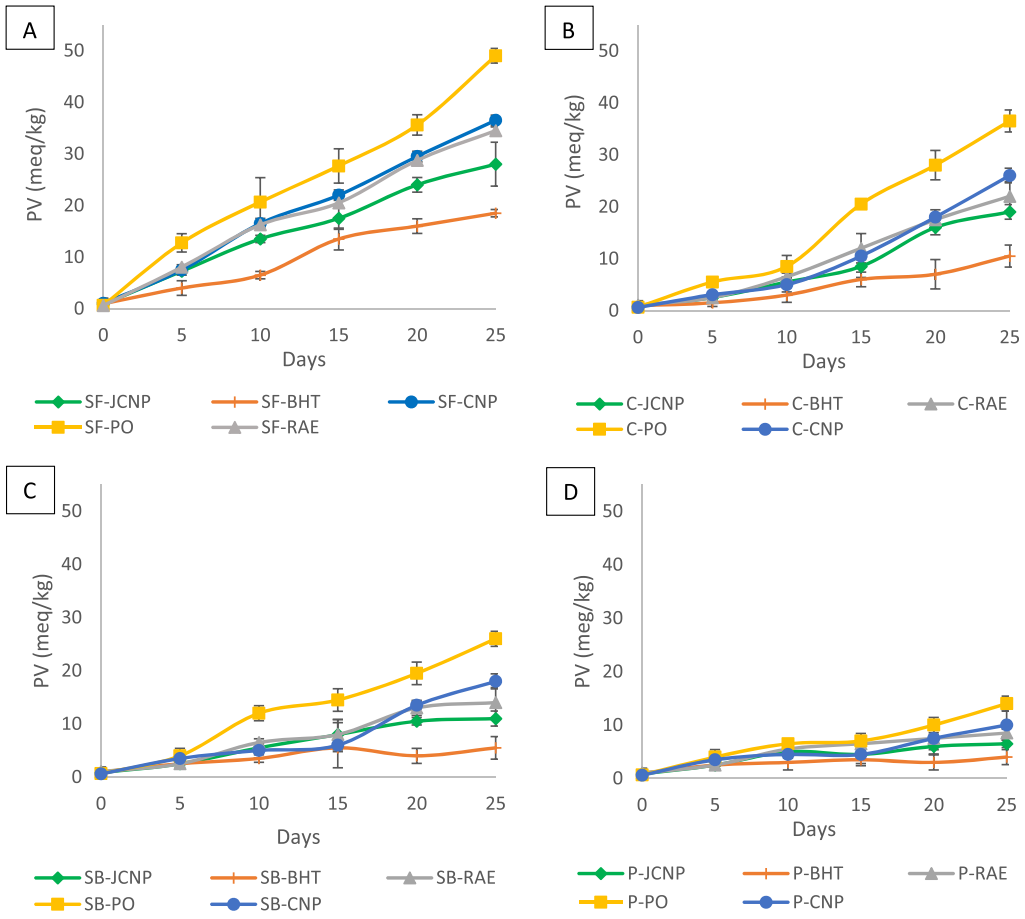

Figure 3. PV of (A) sunflower oil, (B) corn oil, (C) soybean oil, and (D) palm oil containing additive concentrations at a dose of 300 mg/kg.

JCNP as an Antioxidant in Vegetable Oils. *Peroxide Value.* PV is one of the most important quality control parameters in food systems as it indicates the primary oxidation status.[45] The PV results are plotted in Figure 3A–D for sunflower, corn, soybean, and palm oils, respectively. In general, there was a significant increase in PV in all investigated oil samples subjected to accelerated shelf-life storage conditions ($p < 0.05$), with sunflower oil having the highest PV versus the least being observed in palm oil. In the case of sunflower oil (Figure 3A), the PV of SF-PO reached 49.3 meq/kg after a duration of 25 days. In contrast, the PV of SF-CNP and SF-RAE reached maximum values of 36.5 and 34.5 meq/kg, respectively. Both SF-JCNP and SF-BHT showed the lowest PVs of 28.1 and 18.4 meq/kg, respectively. The PV of P-PO reached a maximum value of 14.9 meq/kg. The PVs of P-CNP and P-RAE were equal to 10.1 and 8.5 meq/kg, respectively. As expected from the other oils' results, the PV of palm oil samples containing JCNP and BHT dropped, reaching 6.9 and 4.4 meq/kg, respectively (Figure 3D). The results revealed that the JCNP considerably reduced the rate of formation of PV and their activity was comparable to that of BHT. All oil samples showed an increase in the PV through time of storage ($p < 0.05$), with such an increase being retarded in the oil samples containing JCNP and BHT, especially in the case of sunflower oil. The addition of JCNP to the four oil types could diminish their oxidation compared to that of the free algal extract, suggesting the improved effect of nanoencapsulation on oil stability, retarding the rate of peroxide formation. These results are in agreement with other investigations that used plant extracts in extending the shelf-life of vegetable oils.[46,47]

Thiobarbituric Acid Value. The TBA test determines the amount of malondialdehyde formation as a major secondary byproduct of lipid oxidation reactions in food samples.[48] The TBA values are plotted in Figure 4A–D for sunflower, corn, soybean, and palm oils, respectively. A significant increase in TBA values in all investigated oil samples under accelerated shelf-life storage conditions was observed ($p < 0.05$), with the largest increase being detected in sunflower oil and the least in palm oil. The TBA values of JCNP samples indicate that nanoencapsulation of *J. rubens*' extract had a positive effect on retarding the oil oxidation reactions. Furthermore, JCNP showed an improved effect on retarding the oils' oxidation when compared to the raw *J. rubens*' extract, confirming that nanoencapsulation of natural algal extracts can retard lipid oxidation. Our results are in agreement with other studies that showed that the lowest TBA value was observed in oil samples containing nanoencapsulated natural plant extracts.[47] The TBA values of all oil samples amended with JCNP ranged from 0.30 to 0.45 mg MDA/kg at a temperature set at 60 °C for 25 days, which is approximately equivalent to 230 days at 25 °C of real-time storage, posing it as an efficient additive to elongate the shelf-life of all oil types having different degrees of unsaturation.[49]

Additionally, the degree of oil oxidation, attained from the PV and TBA values, was related to the degree of unsaturation in oils, with palm oil being the least unsaturated and

https://dx.doi.org/10.1021/acsomega.0c06069
ACS Omega 2021, 6, 5642−5652

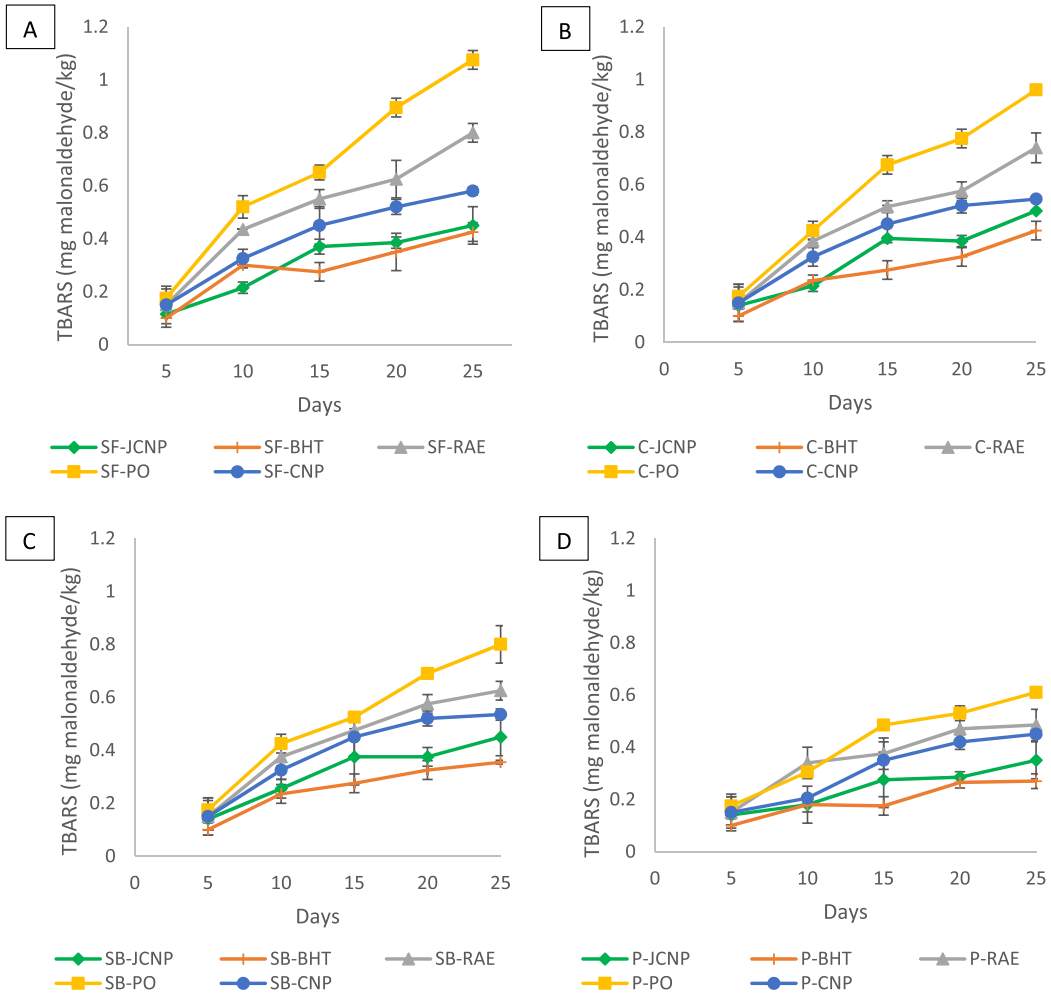

Figure 4. TBA values of (A) sunflower oil, (B) corn oil, (C) soybean oil, and (D) palm oil containing additive concentrations at a dose of 300 mg/kg.

sunflower oil having the highest degree of unsaturation. The results revealed that palm oil showed the least extent of oxidation followed by soybean oil samples, then corn oil samples, and last sunflower oil samples, showing the highest degree of oxidation. These results were in agreement with other investigations that proved that the extent of oil oxidation is dependent on the degree of unsaturation of the different types of oils.[45]

Volatiles as Secondary Markers for Oxidation Analyzed via Headspace Solid-Phase Microextraction. VOCs were used as an index for the oils' oxidation as they comprise a class of chemicals present in most oil types that can indicate rancidity levels.[27] Sunflower oil was used in this investigation as it was the most oxidized among the other oils, as revealed from PV and TBA determinations (Figures 3A and 4A). In addition, it has the highest degree of unsaturation among the other oils studied here, making it more prone to rancidity.[25] The results revealed that aldehydes were the most abundant group of volatiles associated with the rancidity of the oxidized sunflower oil exemplified by pentanal, hexanal, 2-heptanal, octanal, 2-octenal, nonanal, decanal, 2,4-nonadienal, decanal, 2,4-decadienal, undecanal, dodecanal, and (*E*)-2-nonenal and amounting to approximately 52% of the total aroma composition. Alcohols were also produced during the oxidation process represented by isopropyl alcohol and 3-hexe-1-nol.

A comparison between VOCs detected in SF-PO and SF-JCNP is illustrated in Table 2. The fold ratio is equal to SF-PO/SF-JCNP. It was observed that the sunflower oil sample with no additives contained much higher alcohol levels when compared to oil samples with JCNP followed by ketones, alkanes, and aldehydes at fold ratios equal to 18.2, 3.8, 2.7, and 2.1, respectively. Figure 5A–C shows the GC/MS chromatograms of SF-PO, SF-RAE, and SF-JCNP, respectively. It is apparent that the numbers and intensities of the peaks showed an obvious reduction, implying that the rancidity was decreased to a great extent by the addition of JCNP. Specifically, 2,4-decadienal, hexanal, 2-heptanal, nonanal, cyclododecane, and *n*-hexadecanoic acid also showed an obvious reduction with the addition of JCNP. Other investigations studied the oxidation of oils with no additives where aldehydes also amounted as the chief VOCs, including pentanal, hexanal, octanal, nonanal, and 2-heptenal, as reported in the current study.[50,51]

CONCLUSIONS

The ionic gelation method was successfully implemented to produce JCNP with small and uniform PS, high ZP/EE %, and low PDI. Statistical analysis of the 3^3 BBD for PS, ZP,

https://dx.doi.org/10.1021/acsomega.0c06069
ACS Omega 2021, 6, 5642−5652

Table 2. Volatiles Identified in SF-JCNP and SF-PO (Peak Area [×10^6]) with Their Fold Ratios[a]

				average ± SD		
no.	RT (min)	RI	compound name	SF-JCNP	SF-PO	fold ratio
Aldehydes						
1	3.132	702	pentanal		0.34 ± 0.04	
2	4.478	804	hexanal	1.56 ± 0.89	6.12 ± 0.23	3.9
3	6.583	1003	2-heptanal		2.93 ± 0.82	
4	7.149	1018	octanal	0.22 ± 0.13	0.86 ± 0.02	0.2
5	7.659	1055	2-octanal		0.13 ± 0.76	
6	8.309	1112	nonanal	2.57 ± 0.81	2.99 ± 0.11	1.2
7	8.901	1162	(*E*)-2-nonanal		2.71 ± 0.74	
8	9.367	1205	decanal	4.68 ± 0.53	6.42 ± 0.33	1.4
9	9.472	1218	2,4-nonadienal		0.66 ± 0.27	
10	9.928	1265	2-decenal	0.17 ± 0.46	0.33 ± 0.85	1.9
11	10.25	1326	2,4-decadienal	3.99 ± 0.70	5.01 ± 0.67	1.2
12	10.354	1359	undecanal	0.10 ± 0.87	0.52 ± 0.52	5.2
13	10.465	1326	2,4-decadienal	7.83 ± 0.44	14.19 ± 0.03	1.8
14	11.275	1410	dodecanal	0.05 ± 0.66	0.39 ± 0.62	7.8
total aldehydes				21.2	43.6	2.1
Ketones						
15	9.391	1211	thymoquinone	3.65 ± 0.75	11.20 ± 2.22	3.1
16	9.747	1237	2-*sec*-butylcyclohexanone		0.41 ± 0.40	
total ketones				3.7	13.9	3.8
Alcohols						
17	3.585	740	propylene glycol		5.65 ± 2.07	
18	5.234	829	(*Z*)-3-hexen-1-ol	0.88 ± 0.21	2.53 ± 0.11	2.9
19	5.459	909	isopropyl alcohol		6.67 ± 1.83	
20	13.963	1457	3,4-dihydroxyphenylglycol		1.51 ± 0.53	
total alcohols				0.9	16.4	18.2
Alkanes						
21	10.740	1405	pentane,3-ethyl-2,3-dimethyl		2.01 ± 1.21	
22	14.060	1497	cyclododecane	1.86 ± 0.34	3.19 ± 0.34	1.7
total alkanes				1.9	5.2	2.7
Acids						
23	6.778	1001	hexanoic acid		2.34 ± 0.47	
24	10.474	1360	phosphonoacetic Acid		8.63 ± 0.35	
25	16.474	1509	*n*-hexadecanoic acid	2.50 ± 0.11	5.83 ± 0.82	2.3
total acids				2.5	16.8	6.7
Aromatics						
26	10.998	1407	unknown		6.91 ± 2.81	
total aromatics				0	6.9	
Phenols						
27	9.393	1202	*t*-butylhydroquinone		6.02 ± 0.64	
total phenols				0	6.0	

[a]Results are average of two independent replicates (n = 2) ± SD. RT, retention time; RI, Kovats retention index.

PDI, and EE % indicated that the quadratic model was the model of choice. An optimal JCNP formula was prepared and evaluated. It attained a PS of 161 nm, a ZP of 31.2 mV, a PDI of 0.211, and an EE % of 99.7%. The nanoencapsulation of the algal extract improved the antioxidant capacity of the entrapped phytochemicals in vegetable oils. Among the different vegetable oils studied, sunflower oil was the most oxidized type, with JCNP found to effectively mitigate against its oxidation comparable to the widely used synthetic antioxidant BHT, as revealed from the peroxide values, the thiobarbituric acid values, and the headspace VOC analysis. Finally, it was concluded that it is possible to substitute the synthetic antioxidants by natural algal extracts but some forms of encapsulation techniques must be applied in order to protect their properties. The identification of whether the antioxidant effect of *J. rubens* is due to a single component or a synergized action of several phytochemicals in the extract would represent an interesting point for a future study. Additionally, exploring extending the work conducted in this investigation here to other algal species would contribute to the understanding and the potential wider use of nanoencapsulations of such extracts in food preservation applications. Furthermore, the masking of the astringent taste of *J. rubens* will be analyzed via sensory evaluation to prove its applicability in the food industry.

MATERIALS AND METHODS

Materials. Low-molecular-weight chitosan, sodium tripolyphosphate, butylhydroxytoluene, sodium thiosulfate, potassium iodide, a thiobarbituric acid reagent, and a malondialdehyde standard were purchased from Sigma-Aldrich Chemical Co. (St. Louis, USA). (*Z*)-3-Hexenyl acetate

https://dx.doi.org/10.1021/acsomega.0c06069
ACS Omega 2021, 6, 5642−5652

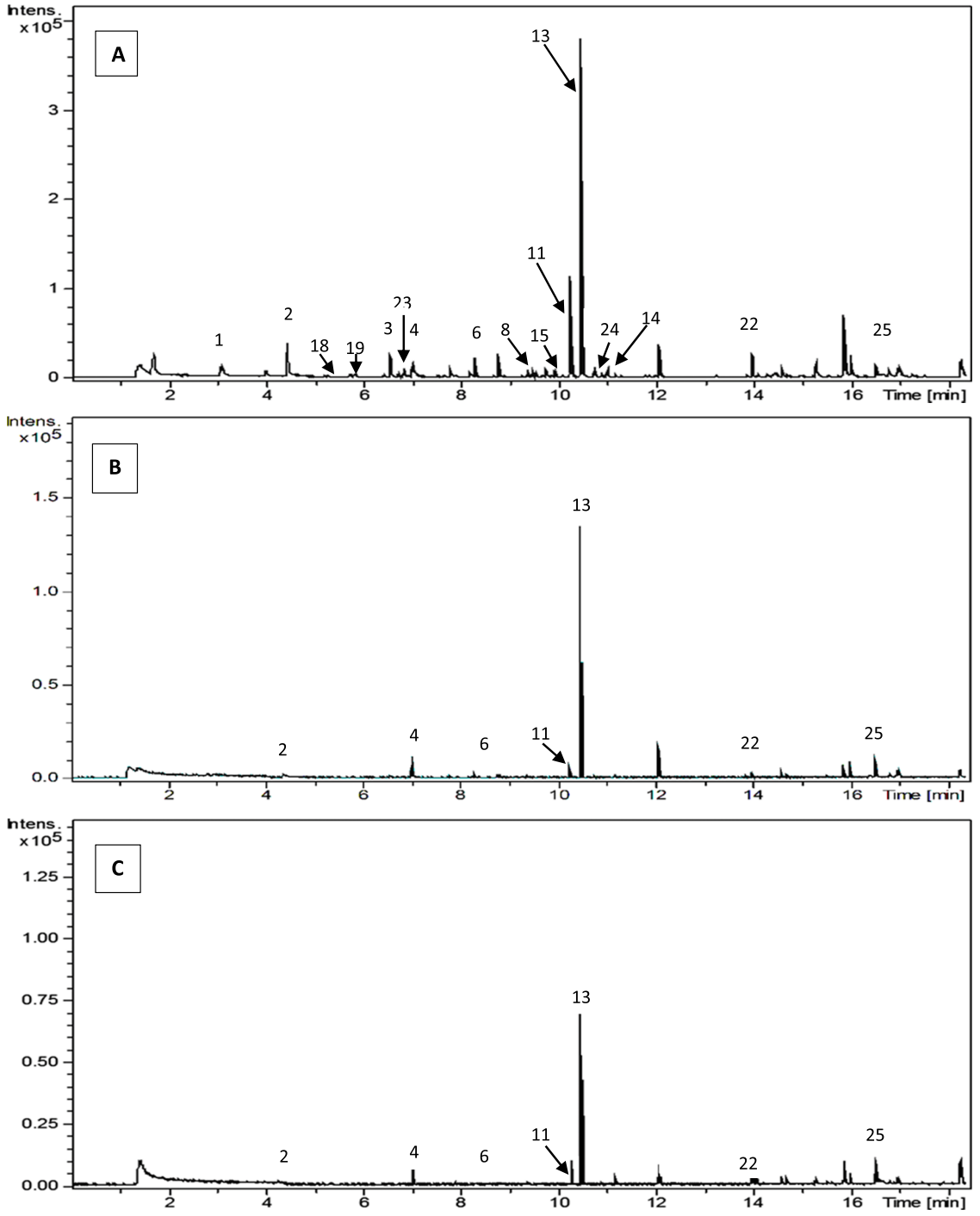

Figure 5. GC chromatogram of (A) SF-PO, (B) SF-RAE, and (C) SF-JCNP with peak numbers following those listed in the table.

volatile standard was purchased from Sigma-Aldrich (Germany). Corn, sunflower, soybean, and palm oils were provided by IFFCO supplier (Suez, Egypt) and used as provided. All other chemicals were of pure analytical grade.

Extraction of Phytochemicals. The extraction of phytochemicals from *J. rubens* was carried out by suspending 20 g of the dried algal powder in 300 mL of 100% ethanol. The mixture was shaken for 48 h at room temperature using a water bath shaker set at 200 rpm. The supernatant was filtered using Whatman filter paper number 1, and the filtrate (9.9 ± 0.59% yield) was evaporated using a rotary evaporator, producing a dry/gummy extract, which was stored at a temperature of −80 °C till further analysis.

Experimental Design. A three-factor, three-level (3^3) BBD was conducted to statistically optimize the variables of JCNP preparation. Construction and estimation of the experimental design were performed using Design Expert software (Version 10, Stat-Ease Inc., Suite 480 Minneapolis, MN 55413). The independent variables were CS percentage (A), TPP percentage (B), HT (C), and HS (D). The levels of factors were selected as (−1, 0, and +1), as shown in Table 1. The dependent variables were chosen as PS (Y1), ZP (Y2), PDI (Y3), and EE % (Y4).

https://dx.doi.org/10.1021/acsomega.0c06069
ACS Omega 2021, 6, 5642−5652

The low and high levels of CS percentage, TPP percentages, HT, and HS were selected based on a preliminary study on the effects of these factors on PS, ZP, PDI, and EE %. Below 0.1% CS and 0.6% TPP, NPs were not sufficiently formed due to the low amounts of CS and TPP available for cross-linking. Levels above 0.4% CS and 1.4% TPP led to unhomogeneous NPs with large PS and PDI. In a previous study conducted by Delan et al.,[21] the selected levels ranged from 0.1 to 0.5% with respect to CS and from 0.4 to 2.0% for TPP. Based on our preliminary study, smaller ranges were studied where the medium levels of the different factors were generated by the software based on the selected low and high levels.

According to the BBD followed design, with three repetitions of the center point per block, 27 formulae were prepared. Each formula was performed twice in two separate replicates for a total of 54 runs. The 27 formulae of the 3^3 BBD with their compositions are shown in Table S3. The estimation of model and term significance was performed by analysis of variance (ANOVA) at p values ($p < 0.05$).

Preparation of JCNP by the Ionic Gelation Technique. Based on the outcome of the BBD, 27 different JCNP formulae were prepared by ionic gelation using TPP as a cross-linking agent.[22] *J. rubens*' extract was dissolved in ethanol (5 mg/0.5 mL). Different weights of CS were dissolved in 9 mL of 1% (v/v) acetic acid at pH 4. An aliquot of 0.5 mL from the freshly prepared algal solution was then added to CS solution, which was stirred at 600 rpm for 15 min. Finally, 1 mL of TPP solution (prepared by dissolving different weights of TPP in distilled water) was added dropwise to the prepared solution during homogenization at different speeds and time durations (UltraTurrax T-25, IKA, Germany). JCNP were then separated by centrifugation (Sigma Laborzentrifugen 1−14, Germany) at 18,000 rpm for 20 min.

PS/PDI Analysis and ZP Measurements. The PS and PDI for all JCNP samples were measured by dynamic light scattering using a Zetasizer (Malvern Instrument Ltd., Worcestershire, UK) operating with a 633 nm laser at 25 °C with an angle of detection of 173°. The electrophoretic mobility measurements were performed at 25 °C for 120 s using a combination of laser Doppler velocimetry and phase analysis light scattering. All measurements were performed in triplicate ± standard deviation (SD).

Determination of EE %. The EE % of all JCNP samples was measured from the clear supernatant obtained after separation of the free algal extract from JCNP by centrifugation at 18,000 rpm for 20 min. The amount of free *J. rubens* was determined by UV−Vis spectrophotometry (CARY 500 SCAN Varian, Hi-tech, USA) at a λ_{max} value of 658 nm using a preconstructed calibration curve ($r^2 = 1$, $n = 3$). The EE % was calculated using the following equation:

$$\text{EE\%} = \frac{(\text{total extract added} - \text{free extract in supernatant})}{\text{total extract added}} \times 100$$

Formulation Optimization. The optimum JCNP was generated using the Design Expert software after applying constraints on PS, ZP, PDI, and EE %, as shown in Table S2, after which the obtained optimum JCNP formula was prepared and measured to assure the validity of the predicted factors and responses of the formulation. For further characterization, the optimum JCNP formula was prepared and lyophilized for 24 h with a condenser temperature of −45 °C (Novalyphe-NL 500, Savant, USA).

Morphological Examination of the Optimal JCNP Formula. The morphology, shape, and size of the optimum JCNP were investigated by TEM (JEOL-JEM2100, Japan). The suspension was added dropwise onto a carbon-coated copper grid. The micrographs' observation was performed at an operating voltage of 200 kV in bright-field mode and by electron diffraction.

Vegetable Oils' Rancidity Determinations. The oil samples were prepared by adding all additives' concentrations at a dose of 300 mg/kg. Four sets were prepared for the four types of oils (i.e. sunflower, corn, soybean, and palm oils). The oil samples were transferred into a series of dark glass bottles, which were placed in an oven at 60 °C for 25 days. PV and TBA values were analyzed every 5 days. A parallel set of samples was prepared and placed in the oven under the same previous conditions to be used for the volatiles' analysis by HS-SPME. All assays were performed in triplicate ± standard deviation (SD).

The PV was determined according to a procedure described elsewhere.[23] Oil samples (3 gm) were dissolved in glacial acetic acid (30 mL) and chloroform (20 mL) (3:2 v/v). Saturated potassium iodide solution (1 mL) was then added. The mixture was shaken for 30 s and then kept in the dark for 1 min. Distilled water (50 mL) was then added followed by titration against sodium thiosulfate (0.01 N). The PV (meq/kg) was calculated using the following equation:

$$\text{PV} = 1000(S \times N)/W$$

where S is the volume of sodium thiosulfate solution (blank corrected) in mL, N is the normality of sodium thiosulfate solution, and W is the weight of oil sample (gm).

TBA was determined according to a procedure described elsewhere.[24] Oil samples (0.2 gm) were dissolved in 25 mL of 1-butanol. Five milliliters of this solution was then mixed with 10 mL of TBA reagent (0.2%) followed by incubation for 2 h in a water bath at 95 °C. The solution was then cooled until it reached room temperature. The absorbance was measured at a λ_{max} value of 532 nm using a UV−Visible spectrophotometer (CARY 500 SCAN Varian, Hi-tech, USA) against a blank (all the reagents except the oil). The TBA value was calculated according to a malondialdehyde preconstructed calibration curve.

HS-SPME was applied on sunflower oil as it was the most oxidized type proven by PV/TBA results, most likely because of its highest degree of unsaturation, rendering it more prone to rancidity.[25] In addition to the prepared samples, fresh unoxidized sunflower oil was analyzed. A total of 250 μL of the oil was placed in a SPME screw cap vial (1.5 mL) and spiked with 10 μg of (*Z*)-3-hexenyl acetate. An SPME fiber was inserted into the vial, which was placed in an oven at 50 °C for 30 min. Divinylbenzene/carboxen/polydimethylsiloxane and polydimethylsiloxane fibers were used. The fiber was subsequently withdrawn into a needle and then injected into the injection port of the gas chromatograph−mass spectrometer (GC/MS). The injector temperature was set at 220 °C. The oven temperature was set at 40 °C for the first 3 min, then increased to 180 °C at a rate of 12 °C min^{-1}, kept at 180 °C for 5 min, finally ramped at a rate of 40 °C min^{-1} to 240 °C, and kept at this temperature for 5 min. Helium carrier gas was used at a flow rate of 0.9 mL/

https://dx.doi.org/10.1021/acsomega.0c06069
ACS Omega 2021, 6, 5642−5652

min.[26] Volatile components were identified by comparing their retention indices relative to *n*-alkanes (C_6–C_{20}) by mass matching to NIST and by comparing them to NIST WILEY library databases. Prior to mass spectral matching, peaks were first deconvoluted using AMDIS software (www.amdis.net).[27]

■ ASSOCIATED CONTENT

Supporting Information

The Supporting Information is available free of charge at https://pubs.acs.org/doi/10.1021/acsomega.0c06069.

Tables of PS, ZP, PDI, and EE %; model summary statistics; and composition of 3^3 BBD (PDF)

■ AUTHOR INFORMATION

Corresponding Author

Yasmin R. Maghraby − *Chemistry Department, The American University in Cairo, New Cairo 11835, Egypt;* orcid.org/0000-0003-1152-4777; Email: ymaghraby@aucegypt.edu

Authors

Mohamed A. Farag − *Chemistry Department, The American University in Cairo, New Cairo 11835, Egypt; Pharmacognosy Department, College of Pharmacy, Cairo University, Cairo 11562, Egypt;* orcid.org/0000-0001-5139-1863

Adham R. Ramadan − *Chemistry Department, The American University in Cairo, New Cairo 11835, Egypt*

Complete contact information is available at: https://pubs.acs.org/10.1021/acsomega.0c06069

Notes

The authors declare no competing financial interest.

■ ACKNOWLEDGMENTS

M.A.F. would like to thank the global public health program, AUC, Egypt for assistance with the GC/MS measurements.

■ ABBREVIATIONS

ANOVA, analysis of variance; BBD, Box–Behnken design; BHT, butylated hydroxy toluene; C-BHT, corn oil with butylated hydroxy toluene; C-CNP, corn oil with chitosan nanoparticles; C-JCNP, corn oil with *Jania rubens* chitosan nanoparticles; C-PO, pure corn oil; C-RAE, corn oil with raw algal extract; CS, chitosan; EE %, encapsulation efficiency; HS, homogenization speed; HS-SPME, headspace solid-phase microextraction; HT, homogenization time; *J. rubens*, *Jania rubens*; JCNP, *Jania rubens* chitosan nanoparticles; NP, nanoparticles; P-BHT, palm oil with butylated hydroxy toluene; P-CNP, palm oil with chitosan nanoparticles; PDI, polydispersity index; P-JCNP, palm oil with *Jania rubens* chitosan nanoparticle; P-PO, pure palm oil; P-RAE, palm oil with raw algal extract; PS, particle size; PV, peroxide value; SB-BHT, soybean oil with butylated hydroxy toluene; SB-CNP, soybean oil with chitosan nanoparticles; SB-JCNP, soybean oil with *Jania rubens* chitosan nanoparticles; SB-PO, pure soybean oil; SB-RAE, soybean oil with raw algal extract; SF-BHT, sunflower oil with butylated hydroxy toluene; SF-CNP, sunflower oil with chitosan nanoparticles; SF-FO, fresh unoxidized sunflower oil; SF-JCNP, sunflower oil with *Jania rubens* chitosan nanoparticles; SF-PO, pure sunflower oil; SF-RAE, sunflower oil with raw algal extract; TBA, thiobarbituric acid; TEM, transmission electron microscopy; TPP, sodium tripolyphosphate; VOC, volatile organic compounds; ZP, zeta potential

■ REFERENCES

(1) Barriuso, B.; Astiasarán, I.; Ansorena, D. A review of analytical methods measuring lipid oxidation status in foods: A challenging task. *Eur. Food Res. Technol.* **2013**, *236*, 1−15.

(2) Varlet, V.; Prost, C.; Serot, T. Volatile aldehydes in smoked fish: Analysis methods, occurence and mechanisms of formation. *Food Chem.* **2007**, *105*, 1536−1556.

(3) Ishakani, A. H.; Joshi, N. H.; Ayaz, M.; Sumara, K.; Vadher, K. H. Antioxidant potential, polyphenols and diphenol content of seaweed available at veraval coast, saurashtra region - Gujarat. *Indian J. Sci. Technol.* **2016**, *9*, 1−6.

(4) Pradhan, N.; Singh, S.; Ojha, N.; Shrivastava, A.; Barla, A.; Rai, V.; Bose, S. Facets of nanotechnology as seen in food processing, packaging, and preservation industry. *Biomed Res. Int.* **2015**, *2015*, 1−17.

(5) Xu, B. J.; Chang, S. K. C. A comparative study on phenolic profiles and antioxidant activities of legumes as affected by extraction solvents. *J. Food Sci.* **2007**, *72*, S159−S166.

(6) Gupta, S.; Abu-Ghannam, N. Bioactive potential and possible health effects of edible brown seaweeds. *Trends Food Sci. Technol.* **2011**, *22*, 315−326.

(7) Farvin, K. H. S.; Jacobsen, C. Phenolic compounds and antioxidant activities of selected species of seaweeds from Danish coast. *Food Chem.* **2013**, *138*, 1670−1681.

(8) Ohara, M.; Ohyama, Y. Delivery and Application of Dietary Polyphenols to Target Organs, Tissues and Intracellular Organelles. *Curr. Drug Metab.* **2014**, *15*, 37−47.

(9) Fayad, S.; Tannoury, M.; Morin, P.; Nehmé, R. Simultaneous elastase-, hyaluronidase- and collagenase-capillary electrophoresis based assay. Application to evaluate the bioactivity of the red alga *Jania rubens*. *Anal. Chim. Acta* **2018**, *1020*, 134−141.

(10) Abdel-raouf, N.; Hozayn, W. G. M.; Ibraheem, I. B. M. *In vivo* application of *Jania rubens* silver nanoparticles as a chemopreventive agent. *Aust. J. Basic Appl. Sci.* **2017**, *11*, 176−186.

(11) Fathi, M.; Varshosaz, J. Novel hesperetin loaded nanocarriers for food fortification: Production and characterization. *J. Funct. Foods.* **2013**, *5*, 1382−1391.

(12) Esmaeili, A.; Asgari, A. *In vitro* release and biological activities of *Carum copticum* essential oil (CEO) loaded chitosan nanoparticles. *Int. J. Biol. Macromol.* **2015**, *81*, 283−290.

(13) Munin, A.; Edwards-Lévy, F. Encapsulation of natural polyphenolic compounds; a review. *Pharmaceutics.* **2011**, *3*, 793−829.

(14) Hu, B.; Liu, X.; Zhang, C.; Zeng, X. Food macromolecule based nanodelivery systems for enhancing the bioavailability of polyphenols. *J. Food Drug Anal.* **2017**, *25*, 3−15.

(15) Bohrey, S.; Chourasiya, V.; Pandey, A. Polymeric nanoparticles containing diazepam: preparation, optimization, characterization, *in-vitro* drug release and release kinetic study. *Nano. Converg.* **2016**, *3*, 1−7.

(16) Fathi, M.; Martín, Á.; McClements, D. J. Nanoencapsulation of food ingredients using carbohydrate based delivery systems. *Trends Food Sci. Technol.* **2014**, *39*, 18−39.

(17) Jain, A.; Thakur, K.; Sharma, G.; Kush, P.; Jain, U. K. Fabrication, characterization and cytotoxicity studies of ionically cross-linked docetaxel loaded chitosan nanoparticles. *Carbohydr. Polym.* **2016**, *137*, 65−74.

(18) Wang, J. J.; Zeng, W. Z.; Xiao, R. Z.; Xie, T.; Zhou, G. L.; Zhan, X. R.; Wang, S. L. Recent advances of chitosan nanoparticles as drug carriers. *Int. J. Nanomed.* **2011**, *6*, 765−774.

(19) Lin, W. C.; Yu, D. G.; Yang, M. C. pH-sensitive polyelectrolyte complex gel microspheres composed of chitosan/sodium tripolyphosphate/dextran sulfate: Swelling kinetics and drug delivery properties. *Colloids Surf., B* **2005**, *44*, 143−151.

https://dx.doi.org/10.1021/acsomega.0c06069
ACS Omega 2021, 6, 5642−5652

(20) Tang, D.-W.; Yu, S.-H.; Ho, Y.-C.; Huang, B.-Q.; Tsai, G.-J.; Hsieh, H.-Y.; Sung, H.-W.; Mi, F.-L. Characterization of tea catechins-loaded nanoparticles prepared from chitosan and an edible polypeptide. *Food Hydrocolloids* **2013**, *30*, 33−41.
(21) Delan, W. K.; Zakaria, M.; Elsaadany, B.; ElMeshad, A. N.; Mamdouh, W.; Fares, A. R. Formulation of simvastatin chitosan nanoparticles for controlled delivery in bone regeneration: Optimization using Box-Behnken design, stability and *in vivo* study. *Int. J. Pharm.* **2020**, *577*, 119038.
(22) Motawi, T. K.; El-Maraghy, S. A.; ElMeshad, A. N.; Nady, O. M.; Hammam, O. A. Cromolyn chitosan nanoparticles as a novel protective approach for colorectal cancer. *Chem.-Biol. Interact.* **2017**, *275*, 1−12.
(23) Mohammadi, A.; Jafari, S. M.; Esfanjani, A. F.; Akhavan, S. Application of nano-encapsulated olive leaf extract in controlling the oxidative stability of soybean oil. *Food Chem.* **2016**, *190*, 513−519.
(24) Uluata, S.; Özdemir, N. Antioxidant activities and oxidative stabilities of some unconventional oilseeds. *J. Am. Oil Chem. Soc.* **2012**, *89*, 551−559.
(25) Masson, L.; Robert, P.; Dobarganes, M. Stability of potato chips fried in vegetable oils with different degree of unsaturation. Effect of ascorbyl palmitate during storage. *Grasas Aceites* **2002**, *53*, 190−198.
(26) Elmassry, M. M.; Kormod, L.; Labib, R. M.; Farag, M. A. Metabolome based volatiles mapping of roasted umbelliferous fruits aroma via HS-SPME GC/MS and peroxide levels analyses. *J. Chromatogr., B: Anal. Technol. Biomed. Life Sci.* **2018**, *1099*, 117−126.
(27) Bencsath, F. A.; Benner, R. A., Jr.; Abraham, A.; Wang, Y.; el Said, K. R.; Jester, E. L. E.; Plakas, S. M. Screening for petrochemical contamination in seafood by headspace solid-phase microextraction gas chromatography-mass spectrometry. *Anal. Bioanal. Chem.* **2015**, *407*, 4079−4090.
(28) Rampino, A.; Borgogna, M.; Blasi, P.; Bellich, B.; Cesàro, A. Chitosan nanoparticles: Preparation, size evolution and stability. *Int. J. Pharm.* **2013**, *455*, 219−228.
(29) Alamdaran, M.; Movahedi, B.; Mohabatkar, H.; Behbahani, M. *In-vitro* study of the novel nanocarrier of chitosan-based nanoparticles conjugated HIV-1 P24 protein-derived peptides. *J. Mol. Liq.* **2018**, *265*, 243−250.
(30) Fan, W.; Yan, W.; Xu, Z.; Ni, H. Formation mechanism of monodisperse, low molecular weight chitosan nanoparticles by ionic gelation technique. *Colloids Surf., B* **2012**, *90*, 21−27.
(31) Hu, B.; Pan, C.; Sun, Y.; Hou, Z.; Ye, H.; Zeng, X. Optimization of fabrication parameters to produce chitosan-tripolyphosphate nanoparticles for delivery of tea catechins. *J. Agric. Food Chem.* **2008**, *56*, 7451−7458.
(32) Ferraris, S.; Cazzola, M.; Peretti, V.; Stella, B.; Spriano, S. Zeta potential measurements on solid surfaces for *in vitro* biomaterials testing : surface charge , reactivity upon contact with fluids and protein absorption. *Front. Bioeng. Biotechnol.* **2018**, *6*, 1−7.
(33) Nallamuthu, I.; Devi, A.; Khanum, F. Chlorogenic acid loaded chitosan nanoparticles with sustained release property, retained antioxidant activity and enhanced bioavailability. *Asian J. Pharm. Sci.* **2015**, *10*, 203−211.
(34) Pulicharla, R.; Marques, C.; Das, R. K.; Rouissi, T.; Brar, S. K. Encapsulation and release studies of strawberry polyphenols in biodegradable chitosan nanoformulation. *Int. J. Biol. Macromol.* **2016**, *88*, 171−178.
(35) Bihari, P.; Vippola, M.; Schultes, S.; Praetner, M. Optimized dispersion of nanoparticles for biological *in vitro* and *in vivo* studies. *Part. Fibre Toxicol.* **2008**, *5*, 14.
(36) Servat-Medina, L.; González-Gómez, A.; Reyes-Ortega, F.; Sousa, I.; Queiroz, N. D.; Zago, P. M.; Jorge, M. P.; Monteiro, K. M.; de Carvalho, J. E.; San Román, J.; Foglio, M. A. Chitosan−tripolyphosphate nanoparticles as *Arrabidaea chica* standardized extract carrier: Synthesis, characterization, biocompatibility, and antiulcerogenic activity. *Int. J. Nanomed.* **2015**, *10*, 3897−3909.
(37) De Oliveira, J. L.; Campos, E. V. R.; Pereira, A. E. S.; Nunes, L. E. S.; Da Silva, C. C.; Pasquoto, T.; Lima, R.; Smaniotto, G.; Polanczyk, R. A.; Fraceto, L. F. Geraniol Encapsulated in Chitosan/Gum Arabic Nanoparticles: A Promising System for Pest Management in Sustainable Agriculture. *J. Agric. Food Chem.* **2018**, *66*, 5325−5334.
(38) Motwani, S.; Chopra, S.; Talegaonkar, S.; Kohli, K.; Ahmad, F. J.; Khar, R. Chitosan-sodium alginate nanoparticles as submicroscopic reservoirs for ocular delivery: Formulation, optimisation and *in vitro* characterisation. *Eur. J. Pharm. Biopharm.* **2008**, *68*, 513−525.
(39) Shukr, M. H.; Ismail, S.; Ahmed, S. M. Development and optimization of ezetimibe nanoparticles with improved antihyperlipidemic activity. *J. Drug Delivery Sci. Technol.* **2019**, *49*, 383−395.
(40) Yadav, S. K.; Khan, G.; Bansal, M.; Vardhan, H.; Mishra, B. Screening of ionically crosslinked chitosan-tripolyphosphate microspheres using Plackett−Burman factorial design for the treatment of intrapocket infections. *Drug Dev. Ind. Pharm.* **2017**, *43*, 1801−1816.
(41) Auwal, S. M.; Zarei, M.; Tan, C. P.; Basri, M.; Saari, N. Enhanced physicochemical stability and efficacy of angiotensin I-converting enzyme (ACE) - Inhibitory biopeptides by chitosan nanoparticles optimized using Box-Behnken design. *Sci. Rep.* **2018**, *8*, 1−11.
(42) Abul Kalam, M.; Khan, A. A.; Khan, S.; Almalik, A.; Alshamsan, A. Optimizing indomethacin-loaded chitosan nanoparticle size, encapsulation, and release using Box-Behnken experimental design. *Int. J. Biol. Macromol.* **2016**, *87*, 329−340.
(43) Patil, P.; Bhoskar, M. Optimization and evaluation of spray dried chitosan nanoparticles containing Doxorubicin. *Int. J. Curr. Pharm. Res.* **2014**, *6*, 7−15.
(44) Shetta, A.; Kegere, J.; Mamdouh, W. Comparative study of encapsulated peppermint and green tea essential oils in chitosan nanoparticles: Encapsulation, thermal stability, *in-vitro* release, antioxidant and antibacterial activities. *Int. J. Biol. Macromol.* **2019**, *126*, 731−742.
(45) Kehili, M.; Choura, S.; Zammel, A.; Allouche, N.; Sayadi, S. Oxidative stability of refined olive and sunflower oils supplemented with lycopene-rich oleoresin from tomato peels industrial by-product, during accelerated shelf-life storage. *Food Chem.* **2018**, *246*, 295−304.
(46) Sayyed-Alangi, S. Z.; Nematzadeh, M. Formulation, development and evaluation of bifunctionalized nanoliposomes containing *Trifolium resupinatum* sprout methanolic extract: As effective natural antioxidants on the oxidative stability of soybean oil. *BMC Chem.* **2019**, *13*, 77.
(47) Savadkouhi, N. R.; Ariaii, P.; Langerodi, M. C. The effect of encapsulated plant extract of *hyssop* (*Hyssopus officinalis L.*) in biopolymer nanoemulsions of *Lepidium perfoliatum* and *Orchis mascula* on controlling oxidative stability of soybean oil. *Food Sci. Nutr.* **2020**, *8*, 1264−1271.
(48) Kaddam, L.; Fadl-Elmula, I.; Eisawi, O.; Abdelrazig, H. Gum Arabic as novel anti-oxidant agent in sickle cell anemia, phase II trial. *BMC Hematol.* **2017**, *17*, 1−6.
(49) Cong, S.; Dong, W.; Zhao, J.; Hu, R.; Long, Y. Characterization of the lipid oxidation process of robusta green coffee beans and shelf life. *Molecules* **2020**, *25*, 1557−1565.
(50) Xu, L.; Yu, X.; Li, M.; Chen, J.; Wang, X. Monitoring oxidative stability and changes in key volatile compounds in edible oils during ambient storage through HS-SPME/GC−MS. *Int. J. Food Prop.* **2018**, *20*, S2926−S2938.
(51) Petersen, K. D.; Kleeberg, K. K.; Jahreis, G.; Fritsche, J. Assessment of the oxidative stability of conventional and high-oleic sunflower oil by means of solid-phase microextraction-gas chromatography. *Int. J. Food Sci. Nutr.* **2012**, *63*, 160−169.

https://dx.doi.org/10.1021/acsomega.0c06069
ACS Omega 2021, 6, 5642−5652